



# Extracellular Vesicles Regulate Sympatho-Excitation by Nrf2 in Heart Failure

Changhai Tian<sup>1</sup>, Lie Gao<sup>2</sup>, Tara L. Rudebush, Li Yu, Irving H. Zucker<sup>2</sup>

**BACKGROUND:** Chronic heart failure (CHF) is associated with redox imbalance. Downregulation of Nrf2 (nuclear factor [erythroid-derived 2]-like 2) plays important roles in disrupting myocardial redox homeostasis and mediating sympathetic nerve activity in the setting of CHF. However, it is unclear if circulating extracellular vesicles (EVs) elicit sympathetic excitation in CHF by disrupting central redox homeostasis. We tested the hypothesis that cardiac-derived EVs circulate to the presympathetic rostral ventrolateral medulla and contribute to oxidative stress and sympathetic excitation via EV-enriched microRNA-mediated Nrf2 downregulation.

**METHODS:** Data were collected on rats with CHF post-myocardial infarction (MI) and on human subjects with ischemic CHF. EVs were isolated from tissue and plasma, and we determined the miRNAs cargo that related to targeting Nrf2 translation. We tracked the distribution of cardiac-derived EVs using in vitro labeled circulating EVs and cardiac-specific membrane GFP<sup>+</sup> transgenic mice. Finally, we tested the impact of exogenously loading of antagomirs to specific Nrf2-related miRNAs on CHF-EV-induced pathophysiological phenotypes in normal rats (eg, sympathetic and cardiac function).

**RESULTS:** Nrf2 downregulation in CHF rats was associated with an upregulation of Nrf2-targeting miRNAs, which were abundant in cardiac-derived and circulating EVs from rats and humans. EVs isolated from the brain of CHF rats were also enriched with Nrf2-targeting miRNAs and cardiac-specific miRNAs. Cardiac-derived EVs were taken up by neurons in the rostral ventrolateral medulla. The administration of cardiac-derived and circulating EVs from CHF rats into the rostral ventrolateral medulla of normal rats evoked an increase in renal sympathetic nerve activity and plasma norepinephrine compared with Sham-operated rats, which were attenuated by exogenously preloading CHF-EVs with antagomirs to Nrf2-targeting miRNAs.

**CONCLUSIONS:** Cardiac microRNA-enriched EVs from animals with CHF can mediate crosstalk between the heart and the brain in the regulation of sympathetic outflow by targeting the Nrf2/antioxidant signaling pathway. This new endocrine signaling pathway regulating sympathetic outflow in CHF may be exploited for novel therapeutics.

**GRAPHIC ABSTRACT:** A graphic abstract is available for this article.

**Key Words:** antioxidant ■ heart failure ■ extracellular vesicles ■ oxidative stress ■ sympathetic nervous system

In This Issue, see p 651 | Meet the First Author, see p 653

An imbalance between pro- and antioxidant signaling pathways contributes to the pathogenesis of the post-myocardial infarction (MI) state and to the progression to chronic heart failure (CHF).<sup>1–3</sup> Nrf2 (nuclear factor [erythroid-derived 2]-like 2) acts as a master transcription factor responsible for the expression of hundreds of antioxidant and anti-inflammatory proteins

in response to oxidative stress. Previous studies have demonstrated that both a global deficiency and selective deletion of Nrf2 in the rostral ventrolateral medulla (RVLM) contribute to pressure overload-induced cardiac hypertrophy and dysfunction and central sympatho-excitation by disrupting redox balance, respectively.<sup>4,5</sup> Conversely, selective overexpression of Nrf2 in the heart and

Correspondence to: Changhai Tian, PhD, Department of Toxicology and Cancer Biology University of Kentucky College of Medicine, Lexington, KY 40536, Email tch815@uky.edu or Irving H. Zucker, PhD, Department of Cellular and Integrative Physiology University of Nebraska Medical Center, Omaha, NE 68198-5850, Email izucker@unmc.edu

Supplemental Material is available at <https://www.ahajournals.org/doi/suppl/10.1161/CIRCRESAHA.122.320916>.

For Sources of Funding and Disclosures, see page 698.

© 2022 American Heart Association, Inc.

Circulation Research is available at [www.ahajournals.org/journal/res](http://www.ahajournals.org/journal/res)

Novelty and Significance

What Is Known?

- Chronic heart failure (CHF) is associated with an increase in sympathetic nerve activity.
- CHF models and human patients both exhibit high levels of oxidative stress in the heart and brain.

What New Information Does This Article Contribute?

- Nrf2 (nuclear factor-erythroid factor 2-related factor 2; a major transcription factor for antioxidant enzyme expression) is reduced in the myocardium and sympathetic regulatory area (rostral ventrolateral medulla) of animals with CHF.
- Specific microRNAs (miRNAs) that target the 3' UTR of Nrf2 are increased in the myocardium and plasma of animals and patients with CHF, as well as extracellular vesicles derived from both cardiac and brain tissues of animals with CHF.
- Transfer of cardiac-derived and circulating extracellular vesicles from CHF rats to the rostral ventrolateral medulla of normal rats resulted in increased sympatho-excitation, which can be attenuated by preloading of CHF-EVs with specific antagonists.

This work demonstrates a unique communication pathway between the injured heart and a specific autonomic regulatory area in the central nervous system. The regulation of pre-sympathetic neuronal discharge in CHF is partly regulated by oxidative stress through Nrf2 signaling. Notably, this regulation is mediated by specific miRNAs contained within plasma and tissue EVs, which are also found in the myocardium and plasma of humans with CHF. Cardiac EVs were demonstrated to be taken up by the central nervous system causing the transference of EVs from CHF rats into normal rats to recapitulate the autonomic phenotype. However, this phenomenon could be abrogated by pre-loading EVs with antagonists to these microRNAs. Overall, these data provide new targets for intervening in the sympatho-excitation of heart failure and potentially other hyper-sympathetic states.

Nonstandard Abbreviations and Acronyms

<b>CHF</b>	chronic heart failure
<b>CO</b>	cardiac output
<b>DH</b>	donor heart
<b>EF</b>	ejection fraction
<b>EV</b>	extracellular vesicle
<b>HO-1</b>	heme oxygenase-1
<b>Keap1</b>	Kelch-like ECH associating protein 1
<b>LVAD</b>	left ventricular assist device
<b>LVEDD</b>	left ventricular end-diastolic diameter
<b>LVEDP</b>	left ventricular end-diastolic pressure
<b>LVEDV</b>	left ventricular end-diastolic volume
<b>LVESD</b>	left ventricular end-systolic diameter
<b>LVESV</b>	left ventricular end-systolic volume
<b>MI</b>	myocardial infarction
<b>miRNA</b>	microRNA
<b>mG</b>	membrane-targeted GFP protein
<b>mT</b>	membrane-targeted tandem dimer Tomato
<b>NC</b>	negative control
<b>Nrf2</b>	nuclear factor (erythroid-derived 2)-like 2
<b>RSNA</b>	renal sympathetic nerve activity
<b>RVLM</b>	rostral ventrolateral medulla
<b>TAM</b>	tamoxifen

in the RVLM suppresses pathological remodeling and sympatho-excitation in mice with CHF by reducing oxidative stress.<sup>6,7</sup> These studies suggest that Nrf2 serves as an important target for modulating cardiac function and autonomic outflow in CHF.

Nrf2 is normally associated with its inhibitory protein Keap1 (Kelch-like ECH associating protein 1) in the cytosol. Under conditions of low or normal oxidative stress, Nrf2 is ubiquitinated and targeted for proteasomal degradation.<sup>8</sup> During abnormally high oxidative stress or in the presence of electrophiles, Nrf2 dissociates from Keap1 and translocates to the nucleus where it binds to antioxidant response elements (AREs) of many genes. microRNAs (miRNAs) have emerged as regulators of cell-cell communication and paracrine signaling mediators in physiological and pathological states by regulating the translation of proteins that are involved in redox homeostasis in the heart and brain.<sup>9–12</sup> miRNAs can circulate, encapsulated in extracellular vesicles (EVs), which are effective carriers and communicators of biological signals (proteins, lipids, and nucleic acids). EVs play critical roles in pathophysiological processes in cardiovascular diseases at local and remote sites (eg, the brain).<sup>13,14</sup> Previous studies have suggested that miRNAs, such as microRNA (miRNA)-27a, miRNA-28a and miRNA-34a can suppress Nrf2 translation by binding to the 3' UTR of Nrf2 mRNA.<sup>15–17</sup> A previous study from this laboratory also showed that these 3 miRNAs

targeting Nrf2 translation were selectively upregulated in the noninfarcted areas of the left ventricle in the rat MI-CHF model. In vitro studies further suggested that these miRNAs can be upregulated in cardiac fibroblasts in response to cardiac stress and subsequently incorporated into EVs and released into the extracellular space where miRNA-enriched EVs directly mediate cardiac myocyte dysfunction by repressing Nrf2 translation.<sup>18</sup>

Accumulating evidence suggests that a reduction of antioxidant enzyme production contributes to oxidative stress in the central nervous system of animals with CHF,<sup>19–21</sup> particularly in the RVLM mediating sympatho-excitation following dysregulation of Nrf2 protein.<sup>6</sup> While this evidence suggests that circulating EVs play an important role in the pathogenesis of the CHF state, it remains unclear if cardiac-derived miRNA-enriched EVs mediate a communication pathway between the heart and the brain and contribute to oxidative stress-mediated sympatho-excitation by targeting Nrf2 signaling in the RVLM.

In the present study, we tested the hypothesis that cardiac-derived EVs evoke sympatho-excitation in the RVLM through EV-miRNAs targeting Nrf2 signaling in CHF and that blockade of these miRNAs would reverse this effect.

## METHODS

### Data Availability

All figures and data tables are available on [www.figshare.com](http://www.figshare.com). The data that support the findings of this study are available from the authors upon reasonable request.

### Rat Model of Chronic Heart Failure

Male Sprague-Dawley rats (180–200 g, 7–8 weeks old) were used for the generation of CHF as previously described.<sup>18,22,23</sup> Briefly, CHF rats underwent permanent left coronary artery ligation, while the Sham rats received the same surgery except for coronary artery ligation. Six weeks post-MI, rats were subjected to echocardiographic analyses to assess cardiac function using the Vevo 3100 Imaging System (Visual Sonics, Inc, Toronto, Canada). Animals that did not develop heart failure following coronary artery ligation were excluded from the heart failure group based on echocardiography analyses. No Sham animals were excluded. Animals with ejection fraction (EF, %) <40% were considered to have systolic dysfunction and heart failure. All experimental protocols were performed as recommended in the NIH Guide for the Care and Use of Laboratory Animals, and approved by the University of Nebraska Medical Center Institutional Animal Care and Use Committee (IACUC).

### Human Subjects

Plasma and myocardial samples from patients with heart failure that received left ventricular assist devices and hearts from normal transplant donors (donor heart [DH]) were provided by the Nebraska Cardiovascular BioBank Registry (NCBR). In brief, patients undergoing an left ventricular assist device

procedure consented before surgery under IRB protocol (133-14-EP). Before surgery or any anticoagulation, venous blood was collected into an EDTA lavender top tube (BD), and then plasma was separated from the red blood cells at 200×g for 10 minutes at RT, and then centrifuged to separate plasma at 1000 to 2000×g for 10 minutes using a refrigerated centrifuge. The plasma samples were then centrifuged for 15 minutes at 5000×g to deplete platelets. The plasma was aliquoted and the supernatant frozen at –80°C until use. The left ventricular core was removed during surgery and was placed into Allprotect Tissue Reagent (Qiagen, Hilden, Germany) and frozen at –80°C as per manufacturer protocol.

## RESULTS

### Heart Failure in Rats

Mean echocardiographic measurements in Sham and CHF rats used in this study are shown in [Figure S1](#). Significant differences were observed for left ventricular end diastolic diameter, left ventricular end systolic diameter, left ventricular end systolic volume, cardiac output, EF, and fractional shortening. Echocardiographic measurements in Sham and CHF rats were performed at various time points (3 wks, 6 wks and 12 wks, post-MI). The results indicate changes in typical heart failure parameters including EF ([Figure S6A](#)), LVEDP ([Figure S6B](#)), LVEDV ([Figure S6C](#)), and LVESV ([Figure S6D](#)) in a time-dependent manner reaching a peak at 6-wk post-MI. Thus, all tissue collections for Western Blotting and qRT-PCR analyses were carried out at 6-wk post-MI.

### Nrf2 Protein Is Dysregulated in the RVLM of Rats With Heart Failure

We measured Nrf2 protein by Western Blotting and qRT-PCR analyses in the RVLM after the nuclei were excised at 6-week post-MI. Data demonstrate that Nrf2 expression was reduced in the RVLM of CHF rats ([Figure 1A](#) and [1B](#)), consistent with previous observations.<sup>6,24</sup> At the same time, there was a significant upregulation of several miRNAs ([Figure 1C](#)) that have been shown to target Nrf2 translation in the CHF group compared with that in the Sham group. Consistently, Nrf2 downstream targets such as HO-1 (heme oxygenase-1; [Figure 1D](#)) and catalase ([Figure 1E](#)) were downregulated. Increased DNA/RNA oxidation stained by 8-OHdG (8-hydroxydeoxyguanosine) antibody ([Figure 1F](#) and [1G](#)) were also observed in the RVLM of rats with CHF compared with Sham rats, indicative of increased oxidative stress.

### Cardiac-Derived EVs Are Enriched With miRNAs That Target Nrf2 Translation

To determine if Nrf2-targeting miRNAs are packaged into EVs and secreted into the extracellular space, we

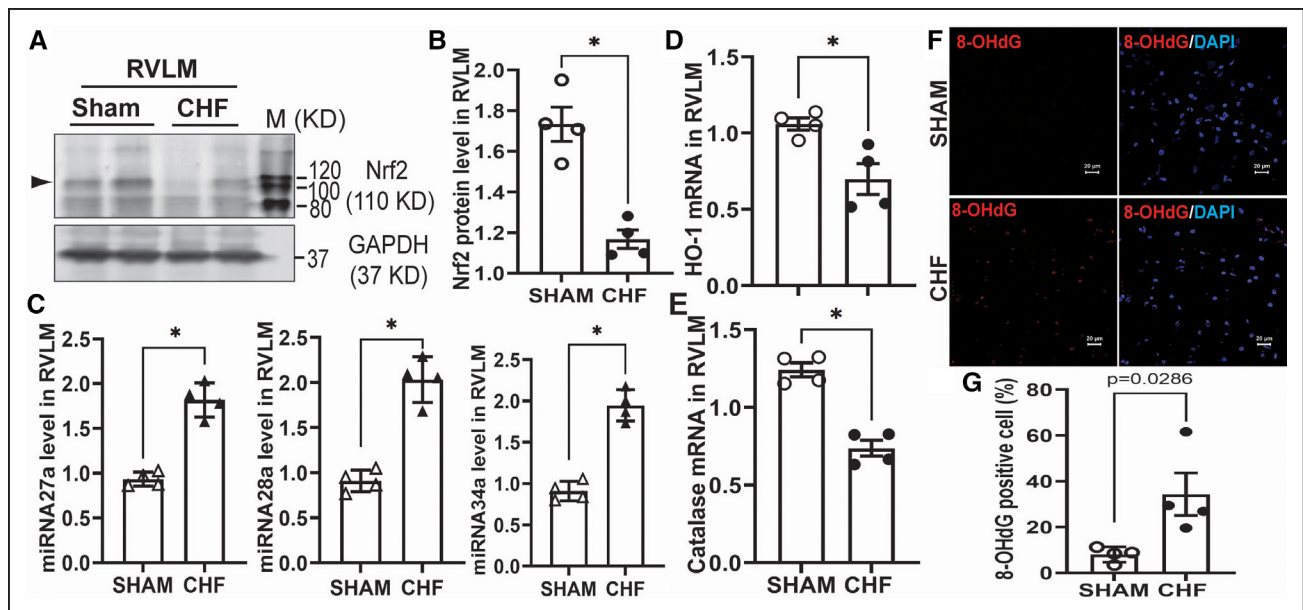


**Figure 1.** Nrf2 (nuclear factor-erythroid factor 2-related factor 2) is dysregulated in the rostral ventrolateral medulla (RVLM) of animals with chronic heart failure (CHF).

Western blots showing Nrf2 expression (as indicated by the arrow) in the RVLM of Sham and CHF rats at 6-week post-MI or Sham surgery (A). Mean data and individual values quantifying Nrf2 expression in Sham and CHF RVLM punches (B); mean and individual values of miRNAs targeting 3'-UTR of Nrf2 mRNA in the RVLM: miR-27a, miR-28a and miR-34a (C) ( $n=4$ ,  $\pm$ SEM); qRT-PCR results show Nrf2 downstream targets, including HO-1 (heme oxygenase 1) mRNA level (D), and catalase mRNA level (E) in RVLM; representative sections of immunostaining with 8-OHdG antibody show DNA/RNA oxidation (F) in the RVLM of Sham (top panel) and CHF (bottom panel) rats, respectively. Summary of the percentages of (G) 8-OHdG-positive cells in the RVLM of Sham ( $n=4$ ) and CHF groups ( $n=4$ ,  $\pm$ SEM). \*Denotes  $P=0.0286$  and all  $P$  were derived using the Mann-Whitney test (nonparametric test). Scale bar is 20  $\mu$ m.

isolated and characterized EVs derived from the myocardium. An example of a transmission electron microscopic image of EVs shows typical cup-shaped morphologies in Figure 2A. The average size ranged from 50 nm to 150 nm (Figure 2B). These cardiac-derived EVs also express typical markers commonly used for EV identification, including CD81, CD9, HSC70, and TSG101 (Figure 2C). Myocardial EVs from the CHF group exhibited significantly higher levels of Nrf2-targeting miRNAs including miRNA-27a (Figure 2D), miRNA-28a (Figure 2E), and miRNA-34a (Figure 2F) compared with that in the Sham group. In addition, cardiac-specific miRNAs including miRNA-1, miRNA-499, and miRNA-208a (Figure 2G through 2I), which are cardiac-specific miRNAs in the myocardium and are involved in cardiogenesis and cardiac function,<sup>25–27</sup> were more abundant in myocardial EVs from CHF rats compared with that from Sham rats. These data suggest that cardiac-derived EVs are enriched with miRNAs targeting Nrf2 translation in the CHF state.

### Circulating EVs Are Elevated in CHF and Are Abundant With miRNAs Targeting Nrf2 Translation

We isolated and characterized plasma-derived EVs from Sham and CHF rats. Typical membrane-bound vesicles were observed in the circulation as indicated by arrows in Figure 3A. The concentration of circulating EVs in CHF

rats were  $\approx 1.5$ -fold higher compared with Sham rats, while there were no differences in size distribution (100–300 nm) (Figure 3B). Further characterization of EVs were carried out by demonstration of expression of EV marker genes, including CD63, CD9, HSC70, and TSG101 (Figure 3C) in both groups. The levels of miRNAs targeting Nrf2 translation, which included miRNA-27a (Figure 3D), miRNA-28a (Figure 3E) and miRNA-34a (Figure 3F), were significantly upregulated in CHF-derived circulating EVs compared with that from Sham rats. Interestingly, cardiac-specific miRNAs (miRNA-1, miRNA-208a, and miRNA-499) were also highly enriched in plasma EVs of CHF rats and reached a peak at 6 wks post-MI compared with that in Sham rats (Figure S7). These data suggest that cardiac-derived Nrf2-targeting miRNAs are packaged into EVs, secreted into the extracellular space entering circulation.

To provide a translational component to these findings, we analyzed the expression of Nrf2-targeting miRNAs in myocardial and plasma samples from patients with ischemic heart disease and heart failure who received left ventricular assist devices (LVAD) and normal unused transplant DH as show in Table S1. qRT-PCR data demonstrated that the levels of Nrf2-targeting miRNAs including miRNA-27a and miRNA-34a were significantly enhanced in myocardial tissues and circulating EVs (Figure S3A, S3C, S3D, and S3F). Although there were no significant alterations of miRNA-28a levels in myocardial tissue and in the circulation between patients with

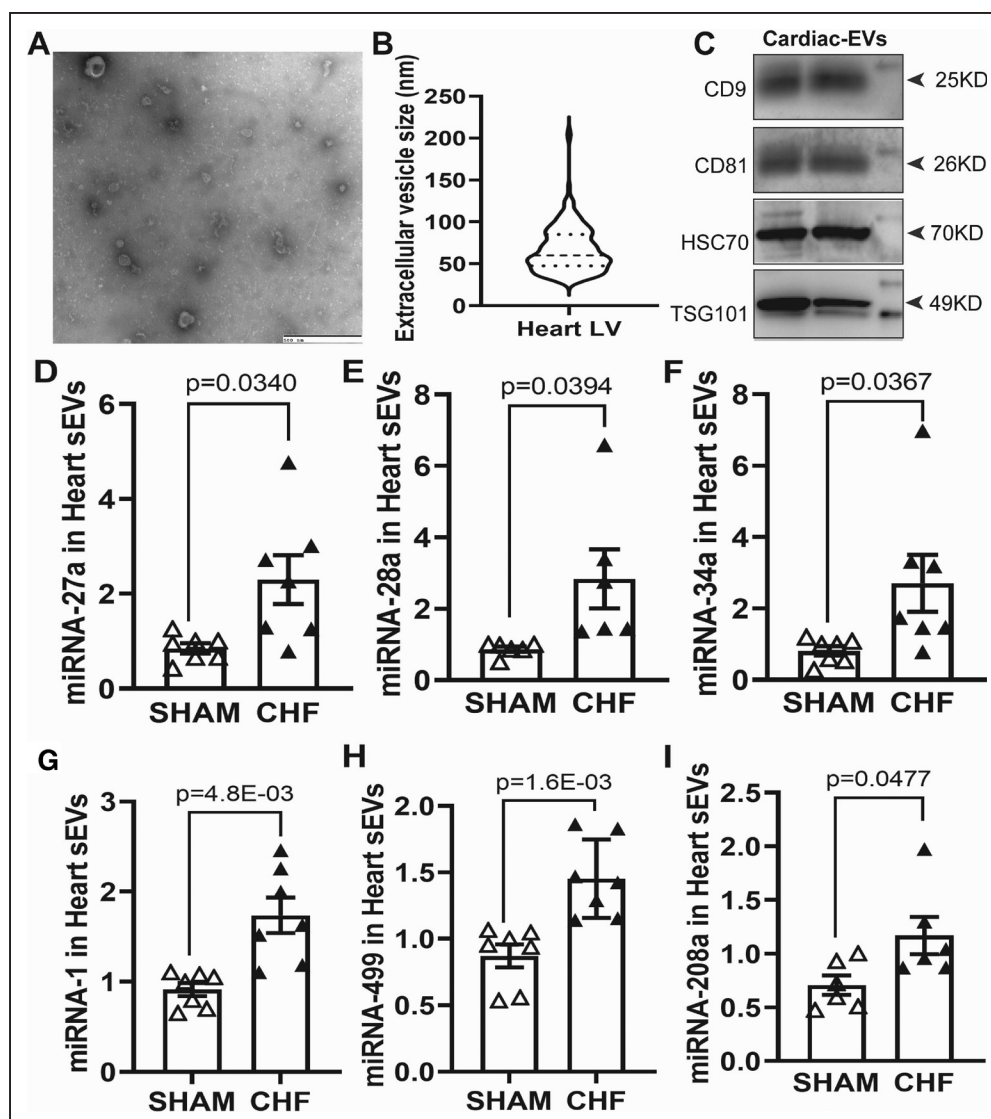


**Figure 2. Cardiac-derived extracellular vesicles (EVs) are abundant with miRNAs targeting Nrf2 (nuclear factor [erythroid-derived 2]-like 2) translation in chronic heart failure (CHF).**

TEM image shows typical morphology of cardiac EVs isolated from the LV of the rat heart (A); EV size was determined by measuring individual EV diameter (nm), and statistical size distribution of LV EVs (B); representative Western blots for CD81, CD9, HSC70, and TSG101 in LV EVs (C); mean and individual data showing miRNAs targeting 3'-UTR of Nrf2 mRNA (miR-27a [D], miR-28a [E], and miR-34a [F]), and cardiac-specific miRNAs (miR-1 [G], miR-499 [H], and miR-208 [I]) were analyzed by real-time qRT-PCR with specific primers, U6 snRNA was used as an internal control ( $n=6$ ,  $\pm$ SEM). Shapiro-Wilk and Kolmogorov-Smirnov test were used to evaluate normality, and  $P$  were derived using an unpaired  $t$  test with Welch correction.

heart failure and normal DH, miRNA-28a levels showed a tendency to increase in the samples from heart failure patients compared with normal DH (Figure S3B and S3E). Consistently, 3 cardiac miRNAs (miRNA-1, miRNA-208a and miRNA-499) also showed a tendency to increase in plasma EVs of patients with ischemic heart failure compared with that in DH (Figure S3G through S3I).

### Circulating EVs Can Pass the Blood-Brain Barrier, Distribute in Brain Tissue and Are Taken up by Neurons in the RVLM

To determine if circulating EVs can enter the brain and be taken up by neurons in the RVLM, we isolated circulating

EVs and labeled them with PKH26 red fluorescent dye. Four hours after intraperitoneal (IP) injection, the RVLM was histologically examined as shown in Figure 4. PKH26<sup>+</sup> EVs were colocalized with MAP2<sup>+</sup> neurons (Figure 4B). The distribution of these EVs within neurons appears to be close to the perinuclear region as seen in higher magnification (Figure 4C). To further confirm the brain distribution of cardiac-derived EVs, we isolated EVs from brain tissues and characterized them by TEM and Western Blotting analysis. The EVs isolated from brain tissues also showed typical EV morphology in both fresh and frozen samples (Figure 5A) without size differences, and size distribution ranged from 50 to 200 nm (Figure 5B). EV markers including CD63, CD9, TSG101, and

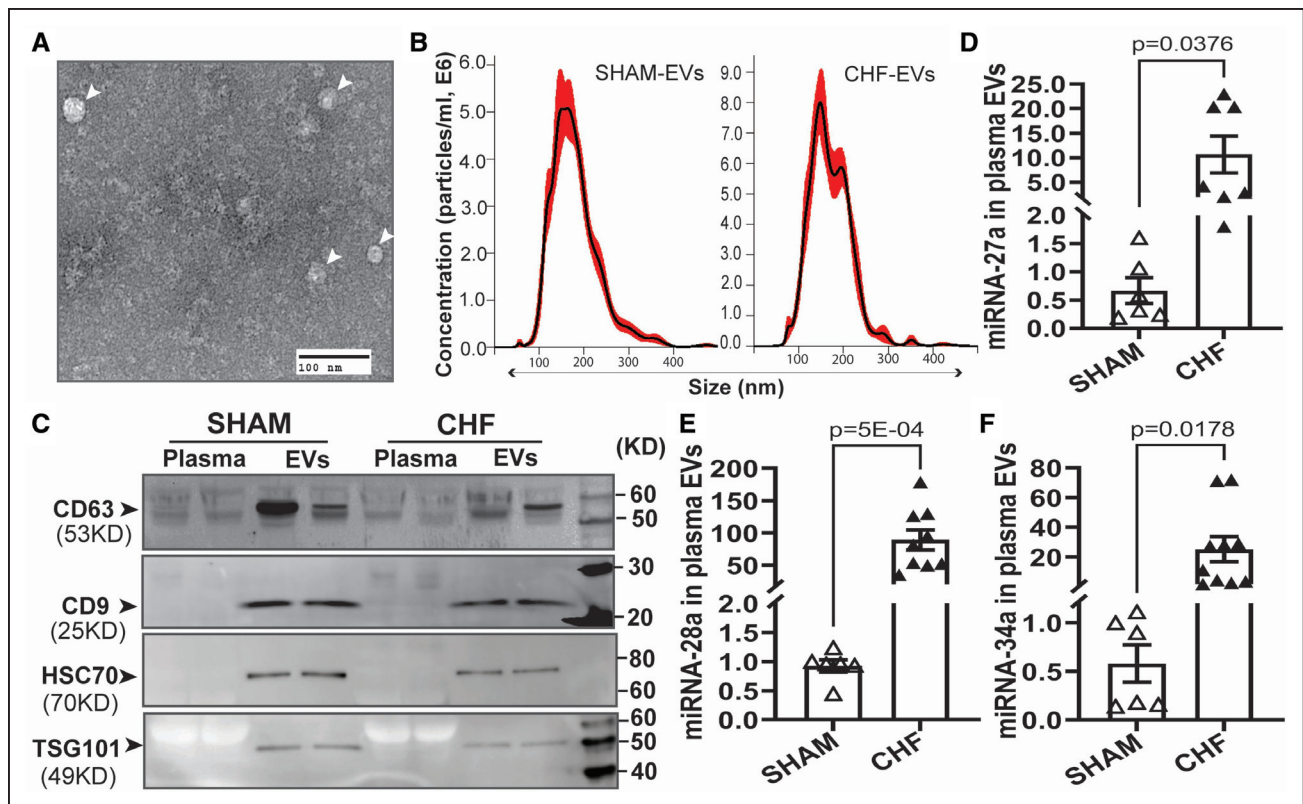


**Figure 3. Plasma extracellular vesicles (EVs) of chronic heart failure (CHF) rats are abundant with Nrf2 (nuclear factor [erythroid-derived 2]-like 2) targeting miRNAs.** EVs isolated from rat plasma by differential centrifugation were subjected to TEM (A), nanosight analysis (B), and Western blot with CD63, CD9, HSC70, and TSG101 antibodies (C); qRT-PCR results show miR-27a (D), miR-28a (E), and miR-34a (F) levels in EVs (Sham: n=6; CHF: n=7;  $\pm$ SEM). Cel-mir-39 was used as a spike-in control. Shapiro-Wilk and Kolmogorov-Smirnov test were used to evaluate normality. *P* were derived using an unpaired *t* test with Welch correction.

HSC70 were also observed in EVs isolated from brain tissues (Figure 5C) indicative of EV stability. Interestingly, we observed that EVs isolated from brain tissue from CHF rats were not only enriched with Nrf2-targeting miRNAs (Figure 5D), but there was enhanced abundance of muscle-enriched (miRNA-1) and cardiac-specific miRNAs (miRNA-208a and miRNA-499, encoded from introns of the heavy chain myosin genes) compared with EVs from Sham rat brains (Figure 5E). These data indicate brain distribution of cardiac-derived EVs, while brain tissue-isolated EVs also contain brain cell-secreted EVs.

To provide further evidence for cardiac derived EVs in the brain, we generated a novel reporter mouse (cardiac-specific membrane GFP<sup>+</sup> mouse) where a global double-fluorescent Cre reporter mouse that expresses membrane-targeted tandem dimer Tomato (mT) before Cre-mediated excision and mG (membrane-targeted GFP protein) was crossed with a myosin heavy chain (Myh6-MerCreMer; tamoxifen (TAM) dependent) transgenic mouse as illustrated in Figure S2A. After TAM administration, these mice underwent MI and Sham-surgery. Six weeks post-MI, there were clear infarcts and fibrosis as seen on the free wall of the left ventricle (indicated by dotted circle in Figure S2B). Echocardiographic images demonstrated a decreased EF (19.4%)

and fractional shortening (8.8%) in the CHF mouse compared with the Sham mouse (EF: 54.4% and fractional shortening: 27.0%; Figure S2E). Fluorescent images of different organs (eg, heart, lung, and brain) by the IVIS imaging system showed that TAM administration specifically switched tdTomato<sup>+</sup> cardiomyocytes to GFP<sup>+</sup> myocytes and GFP<sup>+</sup> signals were also observed in other organs (eg, lung and brain; Figure S2D). GFP signals in the CHF brain was more intense than that in the Sham brain (Figure S2B and S2C), suggesting that cardiomyocyte-derived GFP<sup>+</sup> EVs home to other organs and suggest that MI may cause cardiac GFP<sup>+</sup> EV release and brain distribution. Frozen sections of left ventricles further demonstrated that cardiac myocytes are GFP positive, and nonmyocytes are tdTomato positive in the left ventricles (Figure S2F, upper panel). The population of GFP<sup>+</sup> cardiac myocytes was dramatically decreased and tdTomato<sup>+</sup> signals became stronger post-MI (Figure S2F, bottom panel). Furthermore, we observed that cardiac-derived GFP<sup>+</sup> EVs were not only taken up by neurons in the RVLM of both Sham and CHF mice (Figure S2G) but were also perinuclearly distributed in astrocytes in the cerebral cortex (Figure S2H), further suggesting cross-talk between heart and brain via cardiac-derived EVs.

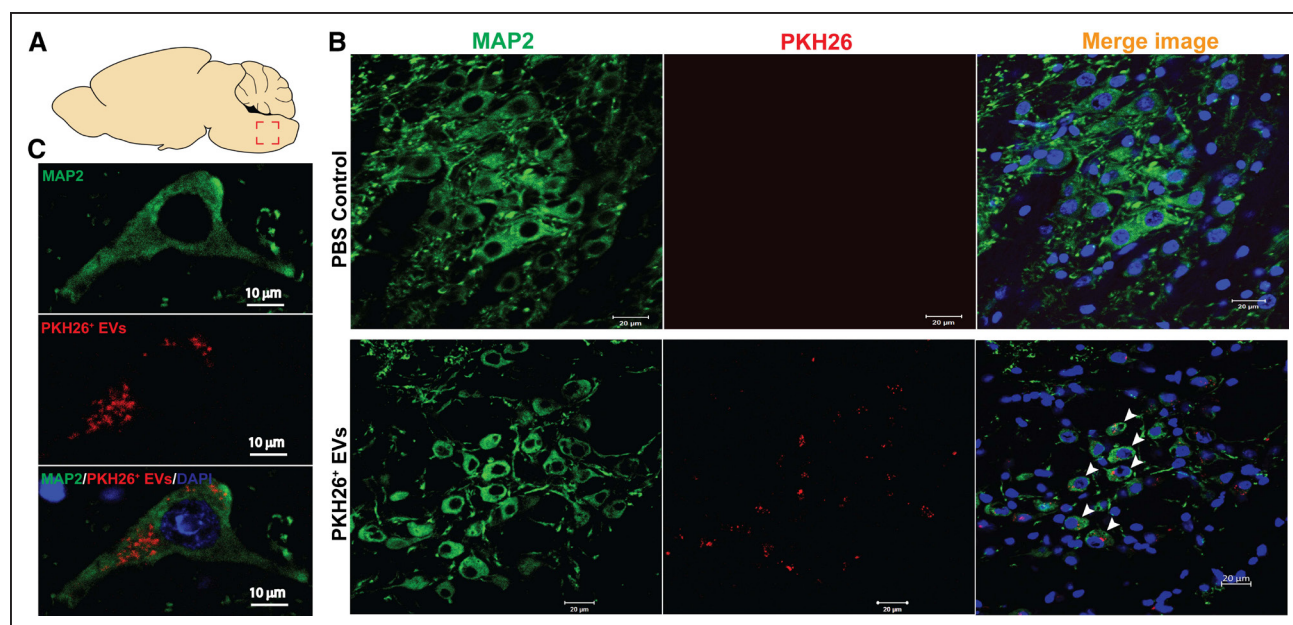


**Figure 4. Circulating extracellular vesicles (EVs) are taken up by neurons in the rostral ventrolateral medulla (RVLM).**

Circulating EVs from rat plasma were labeled with PKH26 Red Fluorescent Cell Linker and administered to mice by IP injection. Four hours post-injection, mice were perfused with ice-cold PBS and 4% PFA, and the brain stem was sectioned in the area shown in the midsagittal section in **A**, and stained with anti-MAP2 antibody and nuclear stained with DAPI. The dashed red rectangular area incorporating the RVLM was screened under confocal microscopy (**B**). Scale bar in **B** is 20  $\mu$ m; EV distribution in neurons in the RVLM are shown at high magnification (**C**). Scale bar is 10  $\mu$ m.

### Cardiac-Derived EVs From HF Rats Transferred to the RVLM Is Associated With Sympatho-excitation in Normal Rats by Dysregulating Nrf2

We have previously demonstrated a reduction of Nrf2 protein and downstream antioxidant enzymes in the RVLM contributing to increased oxidative stress in the central nervous system of animals with CHF.<sup>6</sup> This was also observed in the present study (Figure 1A). To further investigate if circulating EVs contribute to Nrf2 downregulation and subsequent oxidative stress in the RVLM resulting in sympathetic excitation in CHF, we performed bilateral microinjections of circulating EVs exogenously packaged with synthesized miRNA inhibitors (antagomirs targeting miRNA-27a, miRNA-28a, and miRNA-34a at a loading ratio of 1:1:1 into EVs) and negative controls (NC), respectively, into the RVLM of normal rats as schematically illustrated (Figure 6A). Immunofluorescence staining demonstrated that EVs derived from plasma of CHF rats (CHF-EVs) and then transfected with NC decreased Nrf2 protein expression in PKH26<sup>+</sup>/MAP2<sup>+</sup> RVLM neurons, whereas CHF-EVs transfected with antagomirs before microinjection restored Nrf2 protein immunofluorescence (Figure 6B), suggesting that antagomirs functionally block the transcriptional inhibition of Nrf2-targeting miRNAs in the RVLM. Moreover, immunofluorescence indicates increased lipid peroxidation in  $\beta$ III-tubulin<sup>+</sup> neurons that take up PKH26<sup>+</sup> CHF-EVs transfected with NC (CHF-EVs+NC) compared with those neurons

containing PKH26<sup>+</sup> CHF-EVs that were transfected with antagomirs (CHF-EVs+antagomirs; Figure 6C). Furthermore, qRT-PCR results suggest that microinjection of CHF-EV/NC EVs into the RVLM delivers more mature miRNAs targeting Nrf2 translation rather than their precursors (pre-miRNAs; Figure S11) than Sham-EVs/NC whereas these miRNA levels in RVLM were silenced after preloading with antagomirs (Figure S5A through S5C). Consistently, Nrf2 downstream targets in the RVLM including HO-1 and catalase mRNA were downregulated after CHF-EVs/NC microinjection, which were partially restored when CHF-EVs were preloaded with antagomirs before injection (Figure S5D and S5E). These data suggest that CHF-EV-induced oxidative stress in the RVLM was attributed to EV-enriched miRNAs inhibiting the Nrf2 signaling pathway. To specifically determine the effects of cardiac-derived EVs on the expression of Nrf2-targeting miRNAs, pre-miRNAs, and Nrf2 signaling, we isolated myocardial EVs as schematically illustrated in Figure S8A and performed the same procedures as presented in Figure 6A. Subsequently, we observed that cardiac-derived EVs from CHF rats deliver more mature Nrf2-targeting miRNAs rather than pre-miRNAs into RVLM compared with EVs from Sham rats (Figure S12A through S12C and S12G through S12I), contributing to the decrease of Nrf2 signaling, which can be partially recovered by preloading of cardiac-derived CHF-EVs with specific antagomirs (Figure S12D through S12F).

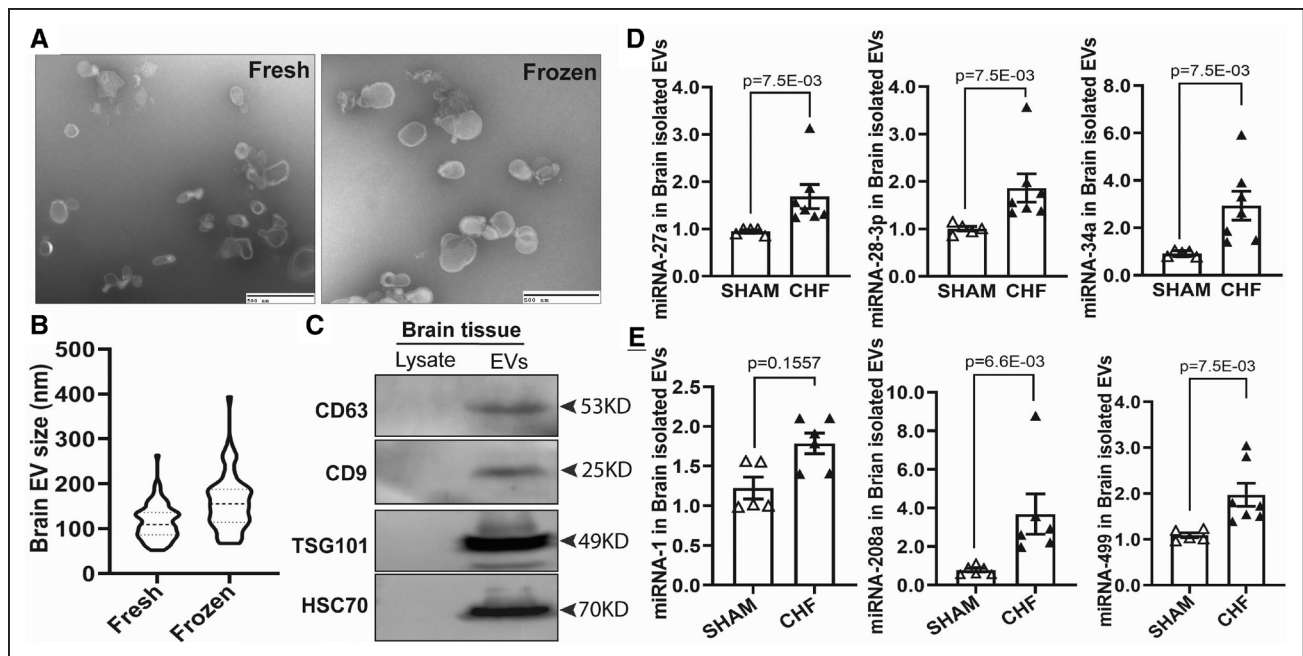


**Figure 5. Cardiac-derived extracellular vesicles (EVs) abundant with miRNAs targeting Nrf2 (nuclear factor [erythroid-derived 2]-like 2) in chronic heart failure (CHF) are distributed to the brain stem.**

The EVs isolated from rat brain by employing enzyme-based methods and differential centrifugation and subjected to TEM (A); EV size was determined by measuring individual EV diameter (nm), and mean values for average size (B) and Western blot analysis with CD63, CD9, TSG101, and HSC70 antibodies (C). qRT-PCR results show the relative expression of miRNAs targeting Nrf2 mRNA (D, Sham: n=5; CHF: n=7;  $\pm$ SEM); Cardiac-specific miRNAs in the EVs isolated from brain (E, Sham: n=5; CHF: n=6;  $\pm$ SEM), D, P were derived by the Mann-Whitney test (nonparametric test) and adjusted using the Bonferroni correction.

In addition, we observed that plasma norepinephrine concentration was significantly increased in rats microinjected with either circulating or cardiac-derived CHF-EVs/NC compared with that in rats microinjected with Sham-EVs/NC. However, the increased norepinephrine levels induced by CHF-EVs were significantly attenuated by preloading of CHF-EVs with antagomirs (Figure 6D; Figure S8B).

To further confirm the pathophysiological effects of both circulating EVs and cardiac-derived EVs on cardiovascular and sympathetic regulation, we performed hemodynamic and renal sympathetic nerve activity (RSNA) recordings and evaluated the arterial baroreflex (acute phenylephrine injection) in anesthetized rats. Original recordings including arterial pressure, heart rate, and RSNA are presented in Figure 7A. There were no significant differences in mean arterial blood pressure (Figure 7B; Figure S8C) and heart rate (Figure 7C; Figure S8D) between groups. In addition, in the circulating EV experimental groups, left-ventricular maximum rate of pressure increases ( $dp/dt_{max}$ ) and decreases ( $dp/dt_{min}$ ) exhibited no significant differences between groups (Figure 7D) while a slight decrease was observed in CHF-EVs compared with the NC group. However, cardiac-derived EVs from CHF rats significantly inhibited the  $dp/dt_{max}$  and  $dp/dt_{min}$  compared with that in rats microinjected with cardiac-EVs of Sham rats, and the effects were slightly restored when CHF-EVs were preloaded with antagomirs (Figure S8E). Consistently,

LVEDP showed significant increases after microinjection of CHF-EVs/NC from both origins compared with Sham-EVs/NC, indicative of a decrease in myocardial performance. However, exogenous preloading of CHF-EVs with antagomirs from both origins significantly attenuated the CHF-EV-elicited LVEDP increase (Figure 7E; Figure S8I). Myocardial EVs from CHF rats evoked a more significant decrease in  $dp/dt_{max}$  and  $dp/dt_{min}$  compared with circulating EVs from CHF rats (Figure 7D; Figure S8E). Preloading of myocardial EVs with antagomirs only partly attenuated cardiac-derived EV-induced LVEDP increase (Figure S8I) compared with the response from circulating EVs (Figure 7E). Baseline RSNA (integrated and normalized) were higher in the CHF-EVs/NC groups compared with that in Sham-EVs/NC groups, whereas the increased RSNA induced by CHF-EVs/NC were significantly attenuated by preloading of these CHF-EVs with antagomirs (Figure 7F; Figure S8F). Notably, the composite arterial baroreflex curves and their first derivative (ie, gain curves) were significantly decreased in CHF-EVs/NC group compared with the Sham-EVs/NC group, whereas preloading with antagomirs into CHF-EVs shifted these physiological alterations toward those of the Sham-EVs/NC group (Figure 7G and 7H; Figure 8G and 8H), suggesting an impairment of baroreflex function in rats given Nrf2-targeting miRNA-enriched EVs into the RVLM, which could be restored by antagomirs silencing Nrf2-targeting miRNAs.

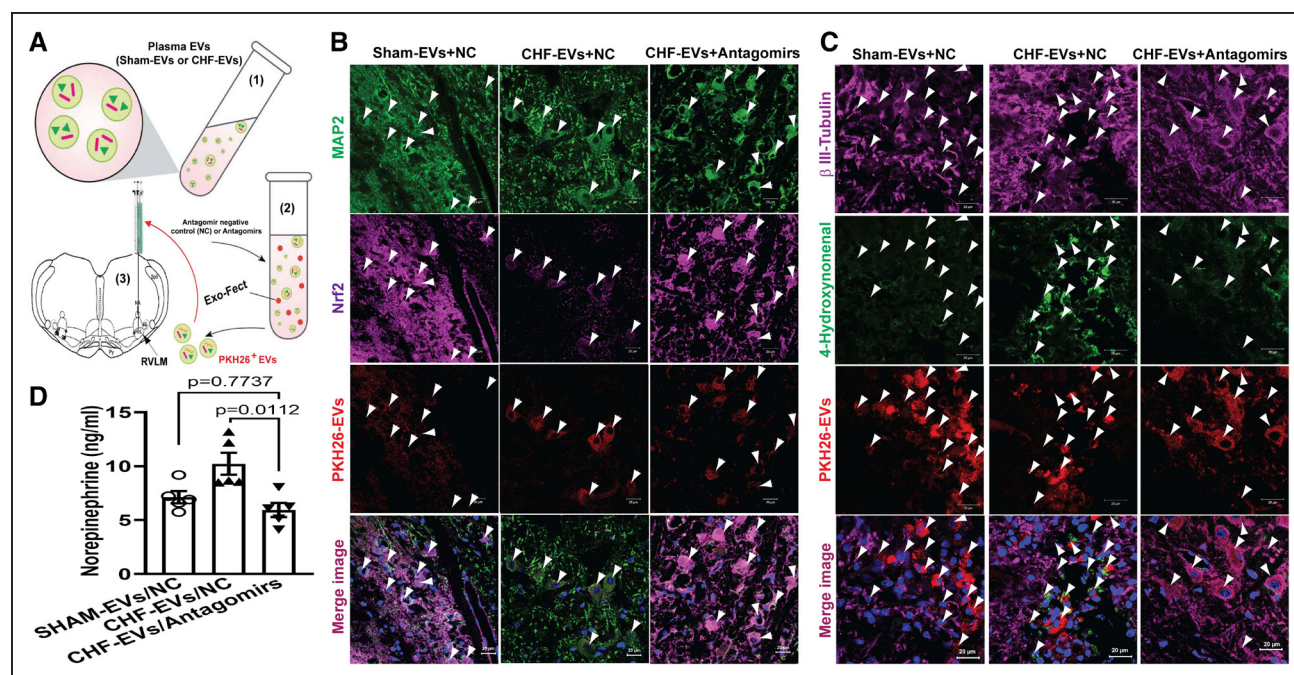


**Figure 6. HF-derived extracellular vesicles (EVs) contribute to Nrf2 (nuclear factor [erythroid-derived 2]-like 2) reduction and oxidative stress in the rostral ventrolateral medulla (RVLM) resulting in sympatho-excitation.**

Schematic diagram for plasma EV isolation, labeling with PKH26, transfection with miRNA negative control and inhibitors, and stereotaxic bilateral microinjection into the RVLM of normal rats (**A**); 3 days post-injection, rats were euthanized and perfused with PBS and 4% PFA. The brain stem was sectioned and subjected to immunostaining with Nrf2 and MAP2 (**B**), and  $\beta$ III-tubulin and 4-HNE antibodies (**C**), respectively. Representative images were used to demonstrate neurons with and without PKH26<sup>+</sup> EVs in the RVLM. Arrows indicate MAP2<sup>+</sup>/Nrf2<sup>+</sup>/PKH26<sup>+</sup> neurons (**B**), and  $\beta$ III-Tubulin<sup>+</sup>/4-HNE<sup>+</sup>/PKH26<sup>+</sup> neurons (**C**). The nuclei were stained with DAPI. Scale bar is 20  $\mu$ m; plasma NE concentration in 3 groups of rats is shown in **D** ( $n=5$ ,  $\pm$ SEM). Statistical analysis was performed using Kruskal-Wallis test, and  $P$  were derived by the Dunn multiple comparisons test.

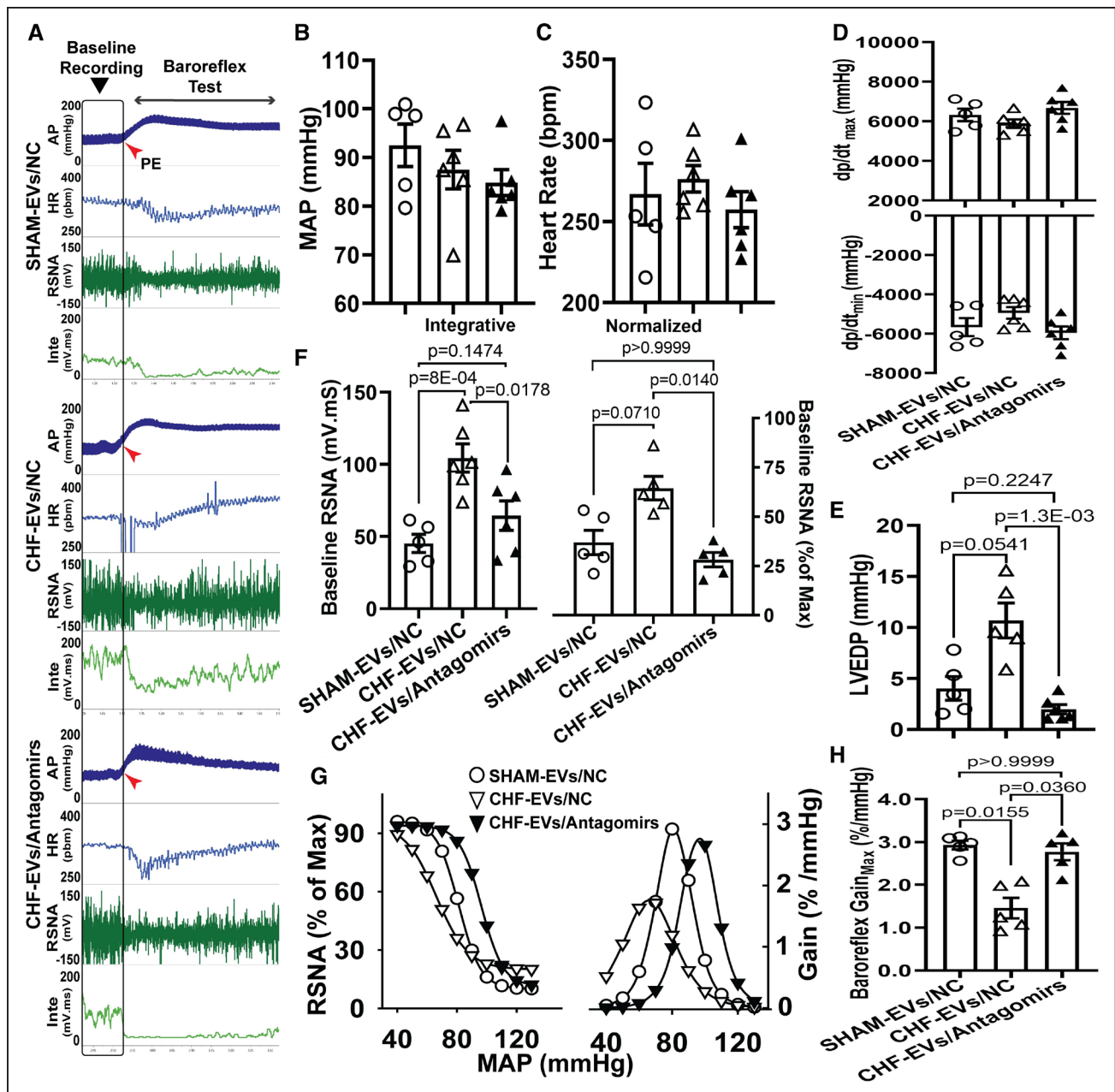
## DISCUSSION

Heart failure is a complex systemic disease that affects almost all tissues to varying degrees. Central nervous system abnormalities are well established in the heart failure syndrome.<sup>28</sup> Previous studies from this laboratory have demonstrated potent abnormalities in autonomic regulation and redox homeostasis in heart failure.<sup>6,21,29</sup> However, the role of cardiac-derived EVs in the brain in heart failure is not well understood.

In the current study, we demonstrated that Nrf2 downregulation in the RVLM of rats with CHF is associated with an upregulation of Nrf2-targeting miRNAs, which are highly enriched in myocardial and circulating EVs (Figures 1 through 3). Our previous studies showed that cardiac fibroblasts upregulate specific miRNAs targeting either Nrf2 signaling or cytoskeletal proteins, which were encapsulated by EVs and secreted into the circulation. Cardiac myocytes underwent oxidative stress and cardiac hypertrophy following uptake of these EVs.<sup>18,22</sup> Although structural and functional alterations associated with CHF are observed primarily in cardiomyocytes and cardiac fibroblasts, the heart has a high degree of cellular and transcriptional diversity.<sup>30,31</sup> Intercellular communications have been well documented.<sup>32–34</sup> This evidence suggests that cardiac-derived EVs play an

important role in the pathogenesis of cell-cell communication in the case of CHF.

Abnormalities in the pathophysiology of the brain in heart failure is also well documented.<sup>35–38</sup> Accumulating evidence has shown that the heart can communicate with the brain via neural and biochemical mechanisms.<sup>35,39</sup> Recently, EVs have emerged as paracrine and endocrine mediators contributing to intra- and inter-organ communication.<sup>32,40–42</sup> Secreted miRNAs, especially those in EVs may mediate communication between different organs and thus modulate gene expression and the function of distant cells and organs.<sup>43</sup> The interactions and communication pathways between the heart and brain are reciprocal. On the one hand, brain injury, such as stroke, can affect cardiac function through neurohumoral mechanisms including circulation of miRNA-enriched EVs.<sup>44</sup> On the other hand, cardiac injury, such as MI causes neuronal damage by increasing the abundance of miRNA-1 in the hippocampus through EVs that are transported from the infarcted heart to the brain.<sup>45</sup> The current study not only further confirms heart-brain crosstalk in CHF (Figures 4 through 5; Figure S2) but also demonstrates a novel mechanism by which cardiac-derived EVs contribute to sympathetic excitation mediated, in part, by neurons in the RVLM (Figures 6 and 7, Figures S5, S8, and S12).



A growing number of studies have demonstrated that extracellular miRNAs not only mediate intercellular communication contributing to pathological cardiac remodeling<sup>32,33,41</sup> but also enter the circulation and potentially act as biomarkers for cardiovascular diseases.<sup>46,47</sup> Clinical studies have also suggested significant alterations of circulating miRNAs in CHF patients,<sup>48,49</sup> potentially serving as diagnostic and prognostic biomarkers for

heart failure. Interestingly, one of the Nrf2-targeting miRNAs, miRNA-27a, was significantly increased in the failing heart compared with the nonfailing heart in humans.<sup>49</sup> Consistently, in the current study, there was also a significant increase of mature miRNA-27a, miRNA-28a, and miRNA-34a observed in EVs derived from the circulation, myocardium, and brain tissue (Figures 2 through 3 and 5), pointing to the clinical and

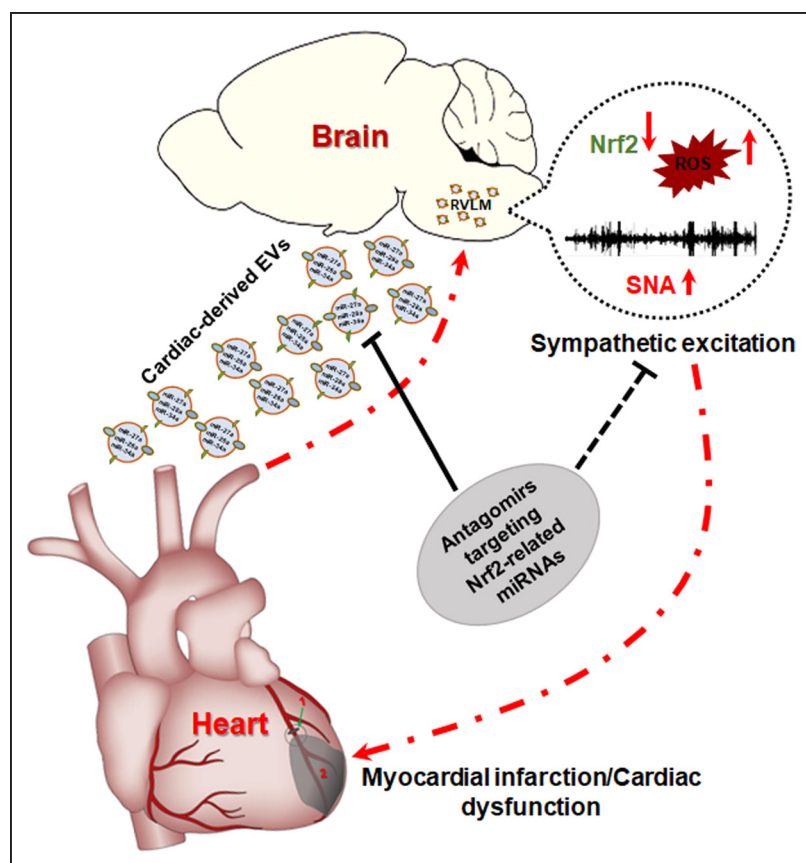


**Figure 8. A schematic overview of a heart-brain communication pathway that modulates central Nrf2 (nuclear factor [erythroid-derived 2]-like 2) and oxidative stress in presympathetic neurons.**

Cardiac-derived extracellular vesicles (EVs) contribute to oxidative stress in the rostral ventrolateral medulla (RVLM) via EV-miRNA-mediated Nrf2 downregulation, resulting in sympathetic excitation and potentially contributing to further cardiac dysfunction. EV loading with antagomirs targeting Nrf2-related miRNAs into chronic heart failure (CHF)-derived EVs attenuates these pathophysiological phenotypes of CHF.

translational relevance of these findings. Using human subject material obtained from the Nebraska Cardiovascular Biobank, we validated that there were also increases in Nrf2-targeting miRNAs in myocardial samples and circulating EVs from patients with ischemic heart failure (Figure S3). These observations are similar to the rat model used here and further support the potential that Nrf2-targeting miRNAs serve as biomarkers and potential therapeutic targets for heart failure.

An important observation of the current study was the transference of pathophysiological phenotypes of CHF by direct RVLM microinjections of CHF-EVs in normal rats. Here, we observed an increase in plasma norepinephrine, an increase in RSNA, and an increase in cardiac LVEDP (Figures 6 and 7; Figure S8), all potentially contributing to cardiac dysfunction and baroreflex impairment. Interestingly, preloading of CHF-EVs with antagomirs silencing Nrf2-targeting miRNAs attenuated these effects, suggesting that Nrf2-targeting miRNAs may be potential therapeutic targets to ameliorate sympatho-excitation in heart failure. Interestingly, circulating CHF-EVs/Antagomirs caused a slight shift in the baroreflex curve compared with Sham-EVs/NC (Figure 7G). Furthermore, HO-1 mRNA level was also slightly increased in the CHF-EVs/Antagomir group (Figure S5D), supporting the possibility that endogenous miRNAs in the RVLM may be silenced by increasing exogenous antagomirs resulting in additional upregulation of Nrf2 signaling, antioxidant

enzymes and decreased oxidative stress in presympathetic neurons. These events contribute to an increase in baroreflex sensitivity and indicate that signaling involving miRNAs and Nrf2 may function under normal conditions in addition to CHF. A limitation in this study is that the effects of Sham-EVs/Antagomirs was not examined. In this study, we not only observed that CHF increased both the amount of miRNA loading in EVs and the number of circulating EVs (Figure 3), but also observed that circulating EVs were predominantly distributed to the brain (Figure S4), suggesting a potential mechanism for enhanced delivery of miRNAs to the RVLM. However, the mechanism by which circulating cardiac-derived EVs target sympatho-regulatory areas in the brain is unknown. In this regard, it is well documented that integrins are highly differentiated in the brain with regional- and cell type-specific expression,<sup>50</sup> and underlie the organotropic metastasis in cancer by entrapping EVs. Consistently, EV distribution to the brain was only observed after intracardiac injection,<sup>51–53</sup> suggesting that integrin patterns may determine the organotropic distribution.

Although oxidative stress in the RVLM has been demonstrated to be responsible for sympatho-excitation in cardiovascular diseases, such as heart failure and hypertension,<sup>54</sup> neuroinflammation in the RVLM also enhances sympathetic excitation and contributes to the pathogenesis of cardiovascular disease.<sup>55</sup> Increasing evidence suggests that in addition to antioxidant activity, Nrf2 also

plays an important role in anti-inflammatory processes either through redox control or by directly suppressing transcriptional upregulation of pro-inflammatory cytokine genes.<sup>56,57</sup> Cardiac-derived EV-mediated Nrf2 downregulation via enriched miRNAs may also contribute to neuroinflammation resulting in sympatho-excitation in the progression of CHF. While not the focus of the present study, this aspect of central redox imbalance remains to be investigated.

## CONCLUSIONS

In this study, male rats were only used to compare the current data with our previous studies and most of the literature. We acknowledge that it is important to evaluate these responses in females in this study and plan to do this in future work. In addition, some of the statistical analyses that should have been corrected for multiple testing may have been overlooked and may be considered a weakness of this study. Although this study demonstrated that cardiac-derived EVs circulate to the brain where they contribute to the dysregulation of Nrf2 signaling, potentially by EV-enriched miRNAs, we did not delineate the cellular origin of these EVs in the progression of CHF in terms of cellular and transcriptional diversity in the heart. In addition, this study was not designed to determine the mechanism by which circulating EVs enter the brain although we observed a predominant brain distribution of exogenously labeled circulating EVs (Figure S4). In this regard and as discussed above, integrins located on EVs may play an important role in determining the organotropism of EVs. This study only focused on Nrf2-regulated redox homeostasis in the RVLM. We used direct microinjection of exogenous EVs into the RVLM to mimic the autonomic phenotype seen in CHF and explored the therapeutic potential of antagomirs to Nrf2-targeting miRNAs. EVs engineered with either directly embedded tissue-specific antibodies or homing peptides *ex vivo* to enhance the delivery efficacy and tissue specificity will represent a promising therapeutic strategy for CHF. Different effects of CHF-EVs/NC on  $dp/dt_{\min/\max}$  were observed between cardiac-derived EVs and circulating EVs, suggesting EV components other than miRNAs may contribute to this difference and remains to be determined. Last, although our human data support the clinical relevance of animal studies, additional human tissue will have to be evaluated to validate the potential of the Nrf2-targeting miRNAs used as biomarkers and therapeutic targets.

In summary, our studies suggest that in post MI-induced CHF, cardiac miRNA-enriched EVs can mediate a heart-brain crosstalk in the regulation of oxidative stress and sympathetic outflow by targeting the Nrf2/antioxidant signaling pathway as schematically illustrated

in Figure 8. These data also suggest a new endocrine signaling pathway regulating sympathetic outflow in CHF that can be exploited for novel therapeutics in several sympatho-excitatory states.

## ARTICLE INFORMATION

Received February 9, 2022; revision received August 17, 2022; accepted August 29, 2022.

### Affiliations

Department of Toxicology and Cancer Biology, University of Kentucky, Lexington, KY. (C.T.). Department of Cellular and Integrative Physiology (T.L.R., L.Y., I.H.Z.) and Department of Anesthesiology (L.G.), University of Nebraska Medical Center, Omaha, NE.

### Acknowledgments

We are grateful to Dr Daniel R. Anderson from the Nebraska Cardiovascular Bio-Bank for providing human samples and the patient donors; Dr Bryan Hackfort from the Echocardiography Imaging Core for echocardiography assessment and analysis; Dr Chi Wang from Division of Cancer Biostatistics of the University of Kentucky College of Medicine for statistical consultation.

### Author Contributions

Conceptualization: C. Tian and I.H. Zucker; C. Tian, L. Gao, and L. Yu performed experiments; T.L. Rudebush provided technical supports for animal studies; data analysis: C. Tian and L. Gao; data discussion: C. Tian, L. Gao, and I.H. Zucker; Article writing: C. Tian, L. Gao, and I.H. Zucker.

### Sources of Funding

This work was supported by the National Institution of Health Grant R01HL153176 to I.H. Zucker/C. Tian and P01 HL62222 to I.H. Zucker; American Heart Association (AHA) Career Development Award (19CDA34520004) to C. Tian. I.H. Zucker was supported, in part, by the Theodore F. Hubbard Foundation.

### Disclosures

None.

### Supplemental Material

Expanded Materials and Methods  
Figures S1–S12  
Tables S1 and S2  
References<sup>58–64</sup>

## REFERENCES

1. Tian C, Gao L, Zhang A, Hackfort BT, Zucker IH. Therapeutic effects of Nrf2 Activation by bardoxolone methyl in chronic heart failure. *J Pharmacol Exp Ther*. 2019;371:642–651. doi: 10.1124/jpet.119.261792
2. Farias JG, Molina VM, Carrasco RA, Zepeda AB, Figueroa E, Letelier P, Castillo RL. Antioxidant therapeutic strategies for cardiovascular conditions associated with oxidative stress. *Nutrients*. 2017;9:E966. doi: 10.3390/nu9090966
3. Bhimaraj A, Tang WH. Role of oxidative stress in disease progression in Stage B, a pre-cursor of heart failure. *Heart Fail Clin*. 2012;8:101–111. doi: 10.1016/j.hfc.2011.08.003
4. Li J, Ichikawa T, Villacorta L, Janicki JS, Brower GL, Yamamoto M, Cui T. Nrf2 protects against maladaptive cardiac responses to hemodynamic stress. *Arterioscler Thromb Vasc Biol*. 2009;29:1843–1850. doi: 10.1161/ATVBAHA.109.189480
5. Gao L, Zimmerman MC, Biswal S, Zucker IH. Selective Nrf2 gene deletion in the rostral ventrolateral medulla evokes hypertension and sympathoexcitation in mice. *Hypertension*. 2017;69:1198–1206. doi: 10.1161/HYPERTENSIONAHA.117.09123
6. Ma A, Hong J, Shanks J, Rudebush T, Yu L, Hackfort BT, Wang H, Zucker IH, Gao L. Upregulating Nrf2 in the RVLM ameliorates sympatho-excitation in mice with chronic heart failure. *Free Radic Biol Med*. 2019;141:84–92. doi: 10.1016/j.freeradbiomed.2019.06.002
7. Shanmugam G, Challa AK, Litovsky SH, Devarajan A, Wang D, Jones DP, Darley-Usmar VM, Rajasekaran NS. Enhanced Keap1-Nrf2

- signaling protects the myocardium from isoproterenol-induced pathological remodeling in mice. *Redox Biol.* 2019;27:101212. doi: 10.1016/j.redox.2019.101212
8. Tian C, Gao L, Zucker IH. Regulation of Nrf2 signaling pathway in heart failure: Role of extracellular vesicles and non-coding RNAs. *Free Radic Biol Med.* 2021;167:218–231. doi: 10.1016/j.freeradbiomed.2021.03.013
  9. Gámez-Valero A, Guisado-Corcoll A, Herrerio-Lorenzo M, Solaguren-Beascoa M, Martí E. Non-coding RNAs as sensors of oxidative stress in neurodegenerative diseases. *Antioxidants (Basel).* 2020;9:E1095. doi: 10.3390/antiox9111095
  10. Chu SF, Zhang Z, Zhou X, He WB, Chen C, Luo P, Liu DD, Ai QD, Gong HF, Wang ZZ, et al. Ginsenoside Rg1 protects against ischemic/reperfusion-induced neuronal injury through miR-144/Nrf2/ARE pathway. *Acta Pharmacol Sin.* 2019;40:13–25. doi: 10.1038/s41401-018-0154-z
  11. Padmavathi G, Ramkumar KM. MicroRNA mediated regulation of the major redox homeostasis switch, Nrf2, and its impact on oxidative stress-induced ischemic/reperfusion injury. *Arch Biochem Biophys.* 2021;698:108725. doi: 10.1016/j.abb.2020.108725
  12. Carbonell T, Gomes AV. MicroRNAs in the regulation of cellular redox status and its implications in myocardial ischemia-reperfusion injury. *Redox Biol.* 2020;36:101607. doi: 10.1016/j.redox.2020.101607
  13. Liu Q, Piao H, Wang Y, Zheng D, Wang W. Circulating exosomes in cardiovascular disease: Novel carriers of biological information. *Biomed Pharmacother.* 2021;135:111148. doi: 10.1016/j.biopha.2020.111148
  14. Sahoo S, Adamiak M, Mathiyalagan P, Kenneweg F, Kafert-Kasting S, Thum T. Therapeutic and diagnostic translation of extracellular vesicles in cardiovascular diseases: roadmap to the clinic. *Circulation.* 2021;143:1426–1449. doi: 10.1161/CIRCULATIONAHA.120.049254
  15. Wang L, Bayanbold K, Zhao L, Wang Y, Adamcakova-Dodd A, Thorne PS, Yang H, Jiang BH, Liu LZ. Redox sensitive miR-27a/b/Nrf2 signaling in Cr(VI)-induced carcinogenesis. *Sci Total Environ.* 2022;809:151118. doi: 10.1016/j.scitotenv.2021.151118
  16. Li N, Muthusamy S, Liang R, Sarojini H, Wang E. Increased expression of miR-34a and miR-93 in rat liver during aging, and their impact on the expression of Mgst1 and Sirt1. *Mech Ageing Dev.* 2011;132:75–85. doi: 10.1016/j.mad.2010.12.004
  17. Yang M, Yao Y, Eades G, Zhang Y, Zhou Q. MiR-28 regulates Nrf2 expression through a Keap1-independent mechanism. *Breast Cancer Res Treat.* 2011;129:983–991. doi: 10.1007/s10549-011-1604-1
  18. Tian C, Gao L, Zimmerman MC, Zucker IH. Myocardial infarction-induced microRNA-enriched exosomes contribute to cardiac Nrf2 dysregulation in chronic heart failure. *Am J Physiol Heart Circ Physiol.* 2018;314:H928–H939. doi: 10.1152/ajpheart.00602.2017
  19. Lindley TE, Infanger DW, Rishniw M, Zhou Y, Doobay MF, Sharma RV, Davison RL. Scavenging superoxide selectively in mouse forebrain is associated with improved cardiac function and survival following myocardial infarction. *Am J Physiol Regul Integr Comp Physiol.* 2009;296:R1–R8. doi: 10.1152/ajpregu.00078.2008
  20. Gao L, Wang W, Liu D, Zucker IH. Exercise training normalizes sympathetic outflow by central antioxidant mechanisms in rabbits with pacing-induced chronic heart failure. *Circulation.* 2007;115:3095–3102. doi: 10.1161/CIRCULATIONAHA.106.677989
  21. Gao L, Wang W, Li YL, Schultz HD, Liu D, Cornish KG, Zucker IH. Superoxide mediates sympathoexcitation in heart failure: roles of angiotensin II and NAD(P)H oxidase. *Circ Res.* 2004;95:937–944. doi: 10.1161/01.RES.0000146676.04359.64
  22. Tian C, Hu G, Gao L, Hackfort BT, Zucker IH. Extracellular vesicular MicroRNA-27a\* contributes to cardiac hypertrophy in chronic heart failure. *J Mol Cell Cardiol.* 2020;143:120–131. doi: 10.1016/j.jmcc.2020.04.032
  23. Gao L, Schultz HD, Patel KP, Zucker IH, Wang W. Augmented input from cardiac sympathetic afferents inhibits baroreflex in rats with heart failure. *Hypertension.* 2005;45:1173–1181. doi: 10.1161/01.HYP.0000168056.66981.c2
  24. Wafi AM, Yu L, Gao L, Zucker IH. Exercise training upregulates Nrf2 protein in the rostral ventrolateral medulla of mice with heart failure. *J Appl Physiol (1985).* 2019;127:1349–1359. doi: 10.1152/japplphysiol.00469.2019
  25. Chistiakov DA, Orekhov AN, Bobryshev YV. Cardiac-specific miRNA in cardiogenesis, heart function, and cardiac pathology (with focus on myocardial infarction). *J Mol Cell Cardiol.* 2016;94:107–121. doi: 10.1016/j.jmcc.2016.03.015
  26. Huang XH, Li JL, Li XY, Wang SX, Jiao ZH, Li SQ, Liu J, Ding J. miR-208a in cardiac hypertrophy and remodeling. *Front Cardiovasc Med.* 2021;8:773314. doi: 10.3389/fcvm.2021.773314
  27. Callis TE, Pandya K, Seok HY, Tang RH, Tatsuguchi M, Huang ZP, Chen JF, Deng Z, Gunn B, Shumate J, et al. MicroRNA-208a is a regulator of cardiac hypertrophy and conduction in mice. *J Clin Invest.* 2009;119:2772–2786. doi: 10.1172/JCI36154
  28. Yancy CW, Jessup M, Bozkurt B, Butler J, Casey DE Jr, Drazner MH, Fonarow GC, Geraci SA, Horwich T, Januzzi JL, et al; American College of Cardiology Foundation; American Heart Association Task Force on Practice Guidelines. 2013 ACCF/AHA guideline for the management of heart failure: a report of the American College of Cardiology Foundation/American Heart Association Task Force on Practice Guidelines. *J Am Coll Cardiol.* 2013;62:e147–e239. doi: 10.1016/j.jacc.2013.05.019
  29. Gao L, Wang W, Li YL, Schultz HD, Liu D, Cornish KG, Zucker IH. Sympathoexcitation by central ANG II: roles for AT1 receptor upregulation and NAD(P)H oxidase in RVLM. *Am J Physiol Heart Circ Physiol.* 2005;288:H2271–H2279. doi: 10.1152/ajpheart.00949.2004
  30. Litviňuková M, Talavera-López C, Maatz H, Reichart D, Worth CL, Lindberg EL, Kanda M, Polanski K, Heinig M, Lee M, et al. Cells of the adult human heart. *Nature.* 2020;588:466–472. doi: 10.1038/s41586-020-2797-4
  31. Tucker NR, Chaffin M, Fleming SJ, Hall AW, Parsons VA, Bedi KC Jr, Akkad AD, Herndon CN, Arduini A, Papangelis I, et al. Transcriptional and cellular diversity of the human heart. *Circulation.* 2020;142:466–482. doi: 10.1161/CIRCULATIONAHA.119.045401
  32. Martins-Marques T, Hausenloy DJ, Sluijter JPG, Leybaert L, Girao H. Intercellular communication in the heart: therapeutic opportunities for cardiac ischemia. *Trends Mol Med.* 2021;27:248–262. doi: 10.1016/j.molmed.2020.10.002
  33. Videira RF, da Costa Martins PA. Non-coding RNAs in cardiac intercellular communication. *Front Physiol.* 2020;11:738. doi: 10.3389/fphys.2020.00738
  34. Bang C, Antoniadou C, Antonopoulos AS, Eriksson U, Franssen C, Hamdani N, Lehmann L, Moessinger C, Mongillo M, Muhl L, et al. Intercellular communication lessons in heart failure. *Eur J Heart Fail.* 2015;17:1091–1103. doi: 10.1002/ehf.399
  35. Triposkiadis F, Karayannis G, Giamouzis G, Skoularigis J, Louridas G, Butler J. The sympathetic nervous system in heart failure physiology, pathophysiology, and clinical implications. *J Am Coll Cardiol.* 2009;54:1747–1762. doi: 10.1016/j.jacc.2009.05.015
  36. Woo MA, Kumar R, Macey PM, Fonarow GC, Harper RM. Brain injury in autonomic, emotional, and cognitive regulatory areas in patients with heart failure. *J Card Fail.* 2009;15:214–223. doi: 10.1016/j.cardfail.2008.10.020
  37. Ogren JA, Fonarow GC, Woo MA. Cerebral impairment in heart failure. *Curr Heart Fail Rep.* 2014;11:321–329. doi: 10.1007/s11897-014-0211-y
  38. Havakuk O, King KS, Grazette L, Yoon AJ, Fong M, Bregman N, Elkayam U, Kloner RA. Heart Failure-Induced Brain Injury. *J Am Coll Cardiol.* 2017;69:1609–1616. doi: 10.1016/j.jacc.2017.01.022
  39. Hodes A, Lichtstein D. Natriuretic hormones in brain function. *Front Endocrinol (Lausanne).* 2014;5:201. doi: 10.3389/fendo.2014.00201
  40. Huang Z, Xu A. Adipose extracellular vesicles in intercellular and interorgan crosstalk in metabolic health and diseases. *Front Immunol.* 2021;12:608680. doi: 10.3389/fimmu.2021.608680
  41. Fu S, Zhang Y, Li Y, Luo L, Zhao Y, Yao Y. Extracellular vesicles in cardiovascular diseases. *Cell Death Discov.* 2020;6:68. doi: 10.1038/s41420-020-00305-y
  42. Gabisonia K, Khan M, Recchia FA. Extracellular vesicle-mediated bidirectional communication between heart and other organs. *Am J Physiol Heart Circ Physiol.* 2022;322:H769–H784. doi: 10.1152/ajpheart.00659.2021
  43. Mori MA, Ludwig RG, Garcia-Martin R, Brandão BB, Kahn CR. Extracellular miRNAs: from biomarkers to mediators of physiology and disease. *Cell Metab.* 2019;30:656–673. doi: 10.1016/j.cmet.2019.07.011
  44. Chen Z, Venkat P, Seyfried D, Chopp M, Yan T, Chen J. Brain-heart interaction: cardiac complications after stroke. *Circ Res.* 2017;121:451–468. doi: 10.1161/CIRCRESAHA.117.311170
  45. Sun LL, Duan MJ, Ma JC, Xu L, Mao M, Biddyt D, Wang Q, Yang C, Zhang S, Xu Y, et al. Myocardial infarction-induced hippocampal microtubule damage by cardiac originating microRNA-1 in mice. *J Mol Cell Cardiol.* 2018;120:12–27. doi: 10.1016/j.jmcc.2018.05.009
  46. Li J, Salvador AM, Li G, Valkov N, Ziegler O, Yeri A, Yang Xiao C, Meechoovet B, Alsop E, Rodosthenous RS, et al. Mir-30d regulates cardiac remodeling by intracellular and paracrine signaling. *Circ Res.* 2021;128:e1–e23. doi: 10.1161/CIRCRESAHA.120.317244
  47. Zhou R, Wang L, Zhao G, Chen D, Song X, Momtazi-Borojeni AA, Yuan H. Circulating exosomal microRNAs as emerging non-invasive clinical

biomarkers in heart failure: Mega bio-roles of a nano bio-particle. *IUBMB Life*. 2020;72:2546–2562. doi: 10.1002/iub.2396

48. Ovchinnikova ES, Schmitter D, Vegter EL, Ter Maaten JM, Valente MA, Liu LC, van der Harst P, Pinto YM, de Boer RA, Meyer S, et al. Signature of circulating microRNAs in patients with acute heart failure. *Eur J Heart Fail*. 2016;18:414–423. doi: 10.1002/ehf.332
49. Matkovich SJ, Van Booven DJ, Youker KA, Torre-Amione G, Diwan A, Eschenbacher WH, Dorn LE, Watson MA, Margulies KB, Dorn GW 2<sup>nd</sup>. Reciprocal regulation of myocardial microRNAs and messenger RNA in human cardiomyopathy and reversal of the microRNA signature by biomechanical support. *Circulation*. 2009;119:1263–1271. doi: 10.1161/CIRCULATIONAHA.108.813576
50. Wu X, Reddy DS. Integrins as receptor targets for neurological disorders. *Pharmacol Ther*. 2012;134:68–81. doi: 10.1016/j.pharmthera.2011.12.008
51. Hoshino A, Costa-Silva B, Shen TL, Rodrigues G, Hashimoto A, Tesic Mark M, Molina H, Kohsaka S, Di Giannatale A, Ceder S, et al. Tumour exosome integrins determine organotropic metastasis. *Nature*. 2015;527:329–335. doi: 10.1038/nature15756
52. Rak J. Cancer: organ-seeking vesicles. *Nature*. 2015;527:312–314. doi: 10.1038/nature15642
53. Liu Y, Cao X. Organotropic metastasis: role of tumor exosomes. *Cell Res*. 2016;26:149–150. doi: 10.1038/cr.2015.153
54. Tan X, Jiao PL, Sun JC, Wang W, Ye P, Wang YK, Leng YQ, Wang WZ.  $\beta$ -Arrestin1 reduces oxidative stress via Nrf2 activation in the rostral ventrolateral medulla in hypertension. *Front Neurosci*. 2021;15:657825. doi: 10.3389/fnins.2021.657825
55. Wu KL, Chan SH, Chan JY. Neuroinflammation and oxidative stress in rostral ventrolateral medulla contribute to neurogenic hypertension induced by systemic inflammation. *J Neuroinflammation*. 2012;9:212. doi: 10.1186/1742-2094-9-212
56. Kobayashi EH, Suzuki T, Funayama R, Nagashima T, Hayashi M, Sekine H, Tanaka N, Moriguchi T, Motohashi H, Nakayama K, et al. Nrf2 suppresses macrophage inflammatory response by blocking proinflammatory cytokine transcription. *Nat Commun*. 2016;7:11624. doi: 10.1038/ncomms11624
57. Ahmed SM, Luo L, Namani A, Wang XJ, Tang X. Nrf2 signaling pathway: pivotal roles in inflammation. *Biochim Biophys Acta Mol Basis Dis*. 2017;1863:585–597. doi: 10.1016/j.bbadis.2016.11.005
58. Muzumdar MD, Tasic B, Miyamichi K, Li L, Luo L. A global double-fluorescent Cre reporter mouse. *Genesis*. 2007;45:593–605. doi: 10.1002/dvg.20335
59. Paxinos G. *The rat brain in stereotaxic coordinates*. George Paxinos, Charles Watson. Elsevier Academic; 2004.
60. Loyer X, Zlatanova I, Devue C, Yin M, Howangyin KY, Klaihmou P, Guerin CL, Kheloufi M, Vilar J, Zannis K, et al. Intra-cardiac release of extracellular vesicles shapes inflammation following myocardial infarction. *Circ Res*. 2018;123:100–106. doi: 10.1161/CIRCRESAHA.117.311326
61. Leroyer AS, Ebrahimian TG, Cochain C, Récalde A, Blanc-Brude O, Mees B, Vilar J, Tedgui A, Levy BI, Chimini G, et al. Microparticles from ischemic muscle promotes postnatal vasculogenesis. *Circulation*. 2009;119:2808–2817. doi: 10.1161/CIRCULATIONAHA.108.816710
62. Perez-Gonzalez R, Gauthier SA, Kumar A, Levy E. The exosome secretory pathway transports amyloid precursor protein carboxyl-terminal fragments from the cell into the brain extracellular space. *J Biol Chem*. 2012;287:43108–43115. doi: 10.1074/jbc.M112.404467
63. Yelamanchili SV, Lamberty BG, Rennard DA, Morsey BM, Hochfelder CG, Meays BM, Levy E, Fox HS. MiR-21 in extracellular vesicles leads to neurotoxicity via TLR7 signaling in SIV neurological disease. *PLoS Pathog*. 2015;11:e1005032. doi: 10.1371/journal.ppat.1005032
64. Arakawa H, Kawabe K, Sapru HN. Angiotensin-(1-12) in the rostral ventrolateral medullary pressor area of the rat elicits sympathoexcitatory responses. *Exp Physiol*. 2013;98:94–108. doi: 10.1113/expphysiol.2012.067116